Effective traffic-flow assignment strategy on multilayer networks

Lei Gao,[1,4] Panpan Shu,[5] Ming Tang,[2,3,*] Wei Wang,[6,†] and Hui Gao[4]

[1]*College of Information Science and Engineering, Shandong Agricultural University, Taian 271018, China*
[2]*School of Mathematical Sciences, Shanghai Key Laboratory of PMMP, East China Normal University, Shanghai 200241, China*
[3]*Shanghai Key Laboratory of Multidimensional Information Processing, East China Normal University, Shanghai 200241, China*
[4]*Web Sciences Center, University of Electronic Science and Technology of China, Chengdu 610054, China*
[5]*School of Sciences, Xi'an University of Technology, Xi'an 710054, China*
[6]*Cybersecurity Research Institute, Sichuan University, Chengdu 610065, China*

(Received 16 August 2017; published 23 July 2019)

An efficient flow assignment strategy is of great importance to alleviate traffic congestion on multilayer networks. In this work, by considering the roles of nodes' local structures on the microlevel, and the different transporting speeds of layers in the macrolevel, an effective traffic-flow assignment strategy on multilayer networks is proposed. Both numerical and semianalytical results indicate that our proposed flow assignment strategy can reasonably redistribute the traffic flow of the low-speed layer to the high-speed layer. In particular, preferentially transporting the packets through small-degree nodes on the high-speed layer can enhance the traffic capacity of multilayer networks. We also find that the traffic capacity of multilayer networks can be improved by increasing the network size and the average degree of the high-speed layer. For a given multilayer network, there is a combination of optimal macrolevel parameter and optimal microlevel parameter with which the traffic capacity can be maximized. It is verified that real-world network topology does not invalidate the results. The semianalytical predictions agree with the numerical simulations.

DOI: 10.1103/PhysRevE.100.012310

I. INTRODUCTION

Many systems in modern society can be described by complex networks, such as power grids, transportation networks, and social networks [1–4]. Alleviating the traffic congestion on such networked systems is a significant issue, which has been widely studied from the perspective of complex network framework over the past decades [5–17]. Most studies about alleviating congestion have focused on monolayer networks, the results of which revealed that traffic congestion is highly related to the structures of networks [18–20]. Generally, there are three widely used techniques to enhance the throughput of the whole network: (1) modification of network structures [21–25], (2) optimization of traffic resources allocation [26–28], and (3) designing better routing strategies [29–35]. Compared with the first two methods, proposing effective routing strategies seems to be more practical and thus has attracted much interest. Among numerous different kinds of proposed routing strategies, an efficient routing strategy proposed by Yan and his colleagues is widely acknowledged for its simplicity and effectivity [29]. The strategy redistributes the traffic load on central nodes to other noncentral nodes, thus improving the network throughput significantly. Echenique *et al.* proposed a novel traffic awareness protocol by considering the waiting time of packets, in which a node forwards a packet to its neighboring node according to the shortest effective distance [36]. Some scholars also proposed strategies for systems with limited band width [37,38]. Except for the research mentioned above, there are other works from the physics community which derive principled routing algorithms [39,40]. For instance, Yeung *et al.* used the physics of interacting polymers and disordered systems to analyze macroscopic properties of generic path optimization problems and proposed a novel routing algorithm by considering all individual path choices simultaneously [40].

With the adoption of big data, scholars found that many modern systems actually include multiple subsystems and layers of connectivity. These systems can be described as multilayer networks [41], and the dynamics of [42] and on [43–47] multilayer networks are markedly different from those of monolayer networks. As we know, the multilayer structure is well established and specialized in computer networking. For instance, the backbone network is composed of two independently developed layers: the backbone IP bearer network (IP layer) and the backbone optical transport network (optical layer). Therefore, the research of routing on multilayer networks is essential, and the ideal routing can be helpful in optimizing traffic performance of real networks [48–54]. Zhuo *et al.* proposed a traffic model formed by a logical layer and a physical layer. In this model, the logical layer builds on top of the physical layer to send packets to their destination nodes according to a given routing strategy, and the physical layer is only in charge of sending packets from one end of the logical link to the other end [48]. Zhuo *et al.* also proposed a global awareness routing strategy to alleviate congestion and to enhance the utilization ratio of two-layer coupled networks [49]. Jiang *et al.* proposed a link-removal strategy based on the degrees of nodes to modify the logical layer network structure,

*tangminghan007@gmail.com
†wwzqbx@hotmail.com

and the study results demonstrated that the traffic capacity can be exponentially improved several times by removing a fraction of links [50].

Another kind of important systems that can be described as multilayer networks are transportation networks [55,56]. For example, to redistribute the traffic flow on a low-speed transportation network (e.g., railway network), we can build a new high-speed network (e.g., airline network) in the busy regions or between the high-flow stations, and then the two-coupled networks can form a multilayer network. Until recently, some researchers have studied the traffic dynamics on multilayer networks, i.e., how to enhance the traffic capacity of multilayer networks in order to alleviate traffic congestion [57–66]. Interestingly, Solé-Ribalta *et al.* [61] developed a standardized model of transportation on multilayer networks and showed that the structure of multiplex networks can induce congestion on account of the unbalance of shortest paths between layers. Morris and Barthélemy [57] analyzed the traffic on multilayer networks consisted of two layers and showed that network utility relies subtly on the interplay between the coupling and randomness in the source-sink distribution. Du *et al.* explored the influence of transfer costs on the transportation system's capacity, and they found that an optimized allocation of transfer costs is achievable by adopting a particle swarm optimization algorithm to increase the total capacity of the infrastructure [64].

Different from monolayer networks, the structures of multilayer networks bring new challenges when we design effective congestion alleviation strategies. On one hand, the structures of multilayer networks can relieve the traffic congestion of one layer, but it may cause congestion on the other layer at the same time [61]. Although establishing high-speed transportation networks can improve the traffic capacity of low-speed networks, we would be confronted with another problem: how to reasonably redistribute the traffic flow. On the other hand, when designing effective flow assignment strategies, we should take (1) the microlevel structures and (2) the efficiencies of different layers into consideration from the microlevel and macrolevel view, respectively. Previous investigations about traffic congestion on multilayer networks were either mainly focused on the differences between layers [57], or the local structure of nodes within the same layer [60], without taking both of them into consideration. In this work, a traffic-flow assignment strategy on multilayer networks is presented. In our model, the macrolevel parameter α_F controls packet-transporting speed on layer F, and the microlevel parameter β_F determines the preference of packets to be transported via small-degree nodes or large-degree ones on layer F. We find that our flow assignment strategy can redistribute the traffic flow on a low-speed layer to a high-speed layer reasonably, and the traffic capacity of multilayer networks can be effectively enhanced with our strategy. Increasing the network size and average degree of the high-speed layer can enhance the traffic capacity of multilayer networks effectively. For a given multilayer network, there is a combination of optimal macrolevel parameter and microlevel parameter that can maximize its traffic capacity. Numerical results on artificial multilayer networks as well as real-world multilayer networks are consistent with our analysis.

The outline of the paper is as follows. In Sec. II we give a detailed description of our traffic-flow assignment strategy on multilayer networks. In Sec. III we suggest theoretical analysis. In Sec. IV we present our simulation results. Section V summarizes our paper with the results and conclusions.

II. MODEL

A. Network model

The multilayer network considered is composed by two layers with N_A and N_B nodes, respectively. Layer A represent the low-speed network, and layer B is the high-speed network. Generally, the costs of building a high-speed network are far more than that of a low-speed network. Therefore, the size of high-speed network is smaller. For example, in the Railway-Airline coupled networks, the speed (cost) of the airline network is faster (more) than that of the railway network. Thus, the size of the airline network is smaller than that of the railway network, and all airline stations are located at points which can be considered as nodes in the railway network, but not vice versa [67]. For simplicity, we assume that the nodes in the high-speed layer B are a subset of the low-speed layer A [57]. We use the uncorrelated configuration model (UCM) [68] to generate the low-speed layer A and use the Erdö-Rényi (ER) networks [69] to represent the high-speed layer B. The multilayer network is generated as follows: (1) Build layer A using the UCM method with power-law degree distributions $P(k) = \Phi k^{-\gamma}$, where $\Phi = 1/\sum_{k=k_{\min}}^{k_{\max}} k^{-\gamma}$ and γ is the degree exponent. Then we set the size of layer A as N_A, and the minimum degree is $k_{\min} = 2$ and the maximum degree is $k_{\max} = \sqrt{N_A}$. (2) Randomly select N_B ($N_B \leqslant N_A$) nodes in layer A, and match these nodes one-to-one. This means that the two matched nodes v_A^o and v_B^o correspond to actually the same station v^o in two different transporting manners. (3) Construct an ER network as the second layer B by using the selected N_B nodes in step (2), i.e., each pair of these randomly selected nodes are connected with a probability p. According to the above three steps, a multilayer network can be built. Note that every node in layer B has its counterpart node in layer A, but the inverse is not true. We denote the degree distribution of the multilayer network as $P(\overrightarrow{K}) = P(k_A, k_B)$, where k_A and k_B mean the degrees of nodes in layer A and B, respectively. For a node v_A in layer A without counterpart in layer B, we have $k_B = 0$. An illustration of the multilayer network is shown in Fig. 1(a).

B. Traffic model

In our model, we assume that all nodes in layer A are both hosts and routers for generating and transporting packets, whereas the nodes in layer B can only transport packets. We assume that a pair of coupled nodes v_A^o and v_B^o can transport packets through the interlayer edge between different layers with infinity bandwidth and no time consumption. This means that the cost of interlayer edge is zero. For simplicity, each node in the layer A (B) has the same maximum packet-transporting ability C_A (C_B), i.e., each node v_A, if it has no counterpart in layer B, can at most transport C_A packets to its neighbors in layer A at each time step. Otherwise, its

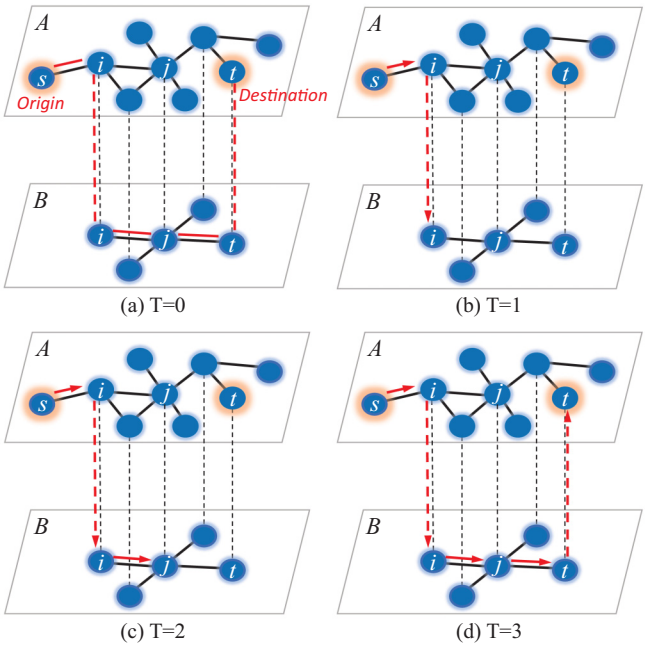

FIG. 1. An illustration of a multilayer network where the nodes of layer B form a subset of the nodes of network A, and nodes in common to both layers are considered to be coupled nodes (indicated as dashed lines). Highlighted in red, a path between the "origin" s and the "destination" t is represented, and the arrows show a packet-transporting process on the path without congestion. A pair of coupled nodes can transport packets between layers without time consumption. (a) At $T = 0$, a packet is generated with the randomly chosen "origin" s and "destination" t in layer A, and a path (highlighted in green) from node s to t is chosen according to the pregiven flow assignment strategy. (b) At $T = 1$, "origin" s transports the packet to the next stop i through the edge (s, i) in layer A. (c) At $T = 2$, node i transports the packet to the next stop j through the edge (i, j) in layer B. (d) At $T = 3$, node j transports the packet to its "destination" t through the edge (j, t) in layer B, and the packet is removed from the system.

counterpart node v_B can also at most transport C_B packets in layer B. We set $C_A = C_B = C = 1$ in this paper for simplicity.

Due to the finite transporting ability of nodes, a queue of buffers is required for each node to accommodate packets waiting to be transported. The transporting process is as follows:

(1) Packet generation: At each time step, R number of packets are generated with randomly chosen origins and destinations in layer A. For each packet, an efficient path from the source to the destination is chosen according to our traffic-flow assignment strategy (to be introduced in the next subsection). If there are several efficient paths between these two nodes, one of them will be randomly selected. Each newly generated packet is placed at the end of the queue of its source node v_A if the next stop is in layer A, or queued at the counterpart node v_B^o if the next stop is in layer B.

(2) Packet processing: The first-in-first-out (FIFO) rule is adopted for each queue. At each time step, coupled nodes v_A^o and v_B^o can process $C_A = C_B = 1$ packet from the heads of their queues and transport the packet to the next stop in layer A and B, respectively. For a noncoupled node v_A (i.e., node v_A has no counterpart node in layer B), it can at most process only $C_A = 1$ packet per time step. When a packet arrives at its destination, it is removed from the system; otherwise it is queued.

C. Traffic flow assignment strategy

By integrating different roles of nodes at the microlevel, as well as different transporting speeds of layers at the macrolevel, we propose a traffic-flow assignment (TFA) strategy. The TFA strategy can reasonably redistribute the traffic flow on the low-speed layer to the high-speed layer and thus improve the traffic capacity of multilayer networks. We denote that a path between nodes s and t as

$$p(s \to t) := s \equiv v_F^0, v_F^1, \ldots, v_F^l, \ldots, v_F^{d-1}, v_F^d \equiv t, \quad (1)$$

where v_F^l is the lst stop and node v_F^l belongs to layer $F \in \{A, B\}$, and d is the number of stops in this path. For any path between nodes s and t, there will be a cost function L, which is defined as

$$L(p(s \to t), \alpha_F, \beta_F) = \sum_{l=0}^{n-1} \alpha_F \left[k\left(v_F^l\right)\right]^{\beta_F}, \quad (2)$$

where $k(v_F^l)$ is the degree of node v_F^l in layer F. We define the "efficient path" between s and t as the route making the cost function $L(p(s \to t), \alpha_F, \beta_F)$ the minimum. If there are several efficient paths between two nodes, we choose one randomly. The efficient path is related to the macrolevel parameter α_F and the microlevel parameter β_F. $\alpha_F \geqslant 0$ controls packet-transporting speed on layer F, and it reflects the difference of transporting speed between layers. The smaller the value of α_F, the faster the transporting speed on layer F. The parameter α_A (α_B) corresponds to the slower (faster) network, and the ratio α_B/α_A controls the relative time required between each jump of transporting through layer B and layer A. β_F determines the preference of packets to be transported through small- or large-degree nodes on layer F, and therefore it can reflect the local structure differences between nodes in the microlevel. Large-degree (small-degree) nodes in layer F are preferentially to be the next stop when $\beta_F < 0$ ($\beta_F > 0$). When $\beta_F = 0$, Eq. (2) returns to the traditionally shortest path (SP) routing strategy. As central nodes (hubs) are congested first in the SP strategy, traffic load on central nodes could be redistributed to other noncentral nodes by setting a positive value of β for monolayer networks [29]. Therefore, we set $\beta_F > 0$ in this paper. In this situation, more packets could be transported through middle-degree nodes. Middle-degree nodes have relatively more connections than small-degree nodes, and meanwhile are not as overloaded as hubs, and therefore the middle-degree nodes would be good routers of packets. The traffic-flow assignment strategy on multilayer networks is illustrated in Fig. 1.

III. THEORETICAL ANALYSIS

From the perspective of statistical physics, we use the order parameter $H(R)$ to characterize the congestion on multilayer networks [29],

$$H(R) = \lim_{t \to \infty} \frac{C}{R} \frac{\langle \Delta W \rangle}{\Delta t}, \quad (3)$$

where $\Delta W = W(t+\Delta t) - W(t)$, $\langle \cdots \rangle$ is the average value over Δt, and $W(t)$ is the total number of accumulated packets in the system at time t. From the varying of H with R, the critical point R_c (to be computed later) can be obtained. For a small value of R (i.e., $R \leqslant R_c$), the number of generated and transported packets are balanced, i.e., every packet can be transported to their destinations in a timely fashion. Thus, $H(R) \to 0$. For a large value of R (i.e., $R > R_c$), the congestion occurs and the number of accumulated packets increases with time. Therefore, $H(R) > 0$. The critical traffic capacity R_c is the most significant parameter of a transportation network, which can be used to evaluate the performance of a flow assignment strategy, i.e., the larger, the better.

To compute the value of R_c, we first define the efficient betweenness centralities (EBC) of nodes in multilayer networks as

$$g(v) = \sum_{s \neq t} \frac{\sigma^{st}(v)}{\sigma^{st}}, \tag{4}$$

where σ^{st} is the number of efficient paths between nodes s and t for given values of α_F and β_F, and $\sigma^{st}(v)$ is the number of efficient paths that pass through node v. In this paper, the efficient paths are obtained from the exhaustive search of paths between every pair of source and destination by using a modified Dijkstra shortest path method, and the computation complexity is about $O(N_A^2)$. The larger value of $g(v)$, the more efficient paths passing through node v. As a result, node v needs to dispose more packets and has a larger probability to be congested. We denote nodes with high values and low values of EBC as high-load (HL) nodes and low-load (LL) nodes, respectively.

A pair of coupled nodes v_A^o and v_B^o can respectively transport the packets to their neighbors in layers A and B, and their values of EBC are $g(v_A^o)$ and $g(v_B^o)$, respectively. Once node v_A^o or v_B^o is overloaded, traffic congestion occurs. Thus, the EBC value of the coupled station v^o is the maximum value of $g(v_A^o)$ and $g(v_B^o)$:

$$g(v^o) = \max\left\{g\left(v_A^o\right), g\left(v_B^o\right)\right\}. \tag{5}$$

For a noncoupled node v_A (i.e., node v_A has no counterpart node in layer B), it can only transport the packets to neighbors in layer A, and its EBC can be expressed as $g(v_A)$.

At every time step, the system will generate R packets in layer A. We can define the average number of packets that a node v needs to process as

$$\langle \Theta_F(v) \rangle = R \frac{g(v)}{N_A(N_A-1)}. \tag{6}$$

When $R \leqslant R_c$, there is no accumulated packets for any node in the system, i.e., $\langle \Theta_F \rangle \leqslant C$. When $R > R_c$, traffic congestion will occur at some HL nodes, i.e., $\langle \Theta_F \rangle > C$. Since the node with the largest EBC value is most likely to be congested, when $C = 1$, the critical packet-generating number R_c should satisfy

$$R_c = \frac{N_A(N_A-1)}{g_{\max}}, \tag{7}$$

where $g_{\max}$ is the largest value of EBC in the system with given α_F and β_F. The value of $g_{\max}$ is obtained by finding the largest value of $g(v)$ in Eq. (4) over all nodes v in a specific network:

$$g_{\max} = \max\{g(v)\}. \tag{8}$$

The theoretical R_c computed from Eq. (7) is called a semianalytical result.

IV. RESULTS

A. Definition of statistical parameters

In simulations, the randomness of traffic dynamics can't ensure that the value of $H(R)$ is equal to zero strictly, while it fluctuates with the order of $1/N_A$ in the free flow state. Therefore, the value of R_c will be identified, once $H(R)$ is greater than $2/N_A$. In addition, four parameters are introduced to investigate the effectiveness of TFA strategy. First, a generalized parameter coupling coefficient based on Ref. [57] is introduced to describe how well two layers are used to transport the packets. Here the coupling coefficient between layers is defined as

$$\lambda = \frac{\sum_{s \neq t} \sigma_B^{st}}{\sum_{s \neq t} \sigma^{st}}, \tag{9}$$

where σ^{st} is the number of efficient paths between nodes s and t for given values of α_F and β_F, and σ_B^{st} is the number of efficient paths that contains at least one edge in layer B. Specifically, we have $\sigma_B^{st} = 0$ when every efficient path between nodes s and t contains only the edges in layer A. For the case of $\lambda = 0$, all packets are transported only by layer A, without using the edges in layer B. With the increase of λ, more packets are transported by using the edges in layer B.

Second, the effective edge ratio δ is introduced as

$$\delta = \frac{\sum_{s \neq t} e_B^{st}}{\sum_{s \neq t} e_A^{st}}, \tag{10}$$

where e_A^{st} (e_B^{st}) is the number of edges belonging to layer A (B) in the efficient paths between nodes s and t for given values of α_F and β_F. When $\delta = 0$, all edges that are used to transport packets belong to layer A. The more edges in layer B are used to transport packets, the larger the value of δ. The definition of λ and δ looks similar. However, they are different in that λ is adopted to represent the proportion of all the efficient paths in the system that contain edges in layer B, and δ refers to the ratio of edges in layer B and A in all efficient paths.

Third, the average length of efficient paths is proposed to measure to capture the effectiveness of the TFA strategy, which can be expressed as

$$\langle d \rangle = \frac{1}{N_A(N_A-1)} \sum_{s \neq t} d^{st}, \tag{11}$$

where d^{st} is length or jumps of efficient paths between node s and t with given values of α_F and β_F. For example, the length of selected path between nodes s and t in Fig. 1 is 3. The smaller the value of $\langle d \rangle$, the fewer average jumps are required for the packets to arrive at the destination.

To improve network traffic capacity, the average delivery time of packets $\langle T \rangle$ must be minimized, where $\langle T \rangle$ is the average time during a packet is generated from its origin and

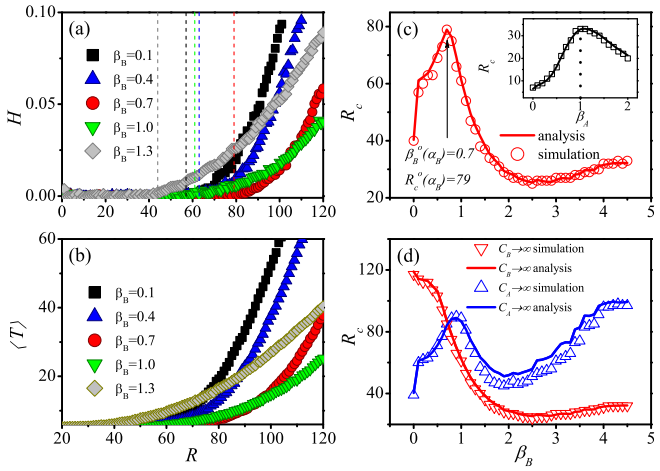

FIG. 2. The performance of TFA strategy on artificial multilayer networks with $\alpha_B = 0.5$. (a) The order parameter H and (b) the average delivery time $\langle T\rangle$ of packets versus R. In panel (a) the dashed lines show the positions of R_c for different β_B, where the order parameter satisfies $H > 2/N_A$ at R_c. (c) The traffic capacity R_c of multilayer networks and (d) the upper limit capacity of layer B (A) as a function of the β_B. The inset of panel (c) is the traffic capacity R_c of monolayer networks (layer A) as a function of β_A when $\alpha_A = 1$. The semianalytical results are obtained from Eq. (6). We set the other parameters as $N_A = 1000$, $\gamma = 3.0$, $k_{\min} = 2$, $k_{\max} = \sqrt{N_A}$, $N_B = 500$, $\langle k_B\rangle = 6$, $\alpha_A = 1$, and $\beta_A = 1$.

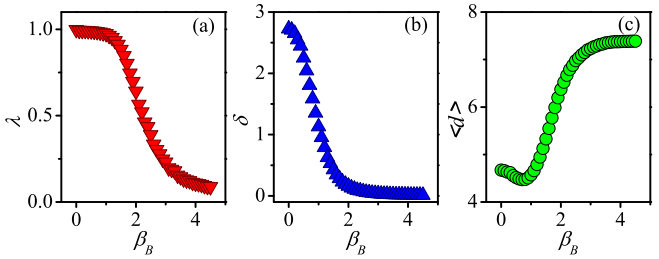

FIG. 3. The parameters (a) the coupling coefficient λ, (b) the effective edge ratio δ, and (c) average length of efficient paths $\langle d\rangle$ vs β_B on artificial multilayer networks. We set the other parameters as $N_A = 1000$, $\gamma = 3.0$, $k_{\min} = 2$, $k_{\max} = \sqrt{N_A}$, $N_B = 500$, $\langle k_B\rangle = 6$, $\alpha_A = 1$, $\beta_A = 1$, and $\alpha_B = 0.5$.

delivered to its destination. The definition of $\langle T\rangle$ is given by

$$\langle T\rangle = \lim_{t\to\infty} \frac{1}{n} \sum_{p=1}^{n} T_p, \tag{12}$$

where n is the number of arrived packets at a given time t and T_p is the delivery time of packet p. The delivery time of each packet consists of the traveling time from the origin to the destination and the waiting time in the queues of nodes. When R is less than R_c, $\langle T\rangle$ depends only on the traveling time, which is relatively small. However, when $R > R_c$, $\langle T\rangle$ increases with R rapidly.

B. Artificial multilayer networks

In this subsection, extensive numerical simulations is executed on artificial multilayer networks. We set the size of layer A as $N_A = 1000$, and degree exponents $\gamma = 3.0$, and the minimum degree $k_{\min} = 2$, and the maximum degree $k_{\max} = \sqrt{N_A}$. The size of layer B is $N_B = 500$ and average degree $\langle k_B\rangle = 6$. All the results are obtained by averaging over 20 different network realizations, with 100 independent runs for each realization.

In Fig. 2 we first focus on exploring the effects of microlevel parameter β_B on the effectiveness of TFA strategy. According to the Ref. [29], $\beta_A \approx 1$ is the optimal value for uncorrelated single-layer networks [see the inset of Fig. 2(c)]. Therefore, we set $\alpha_A = 1$ and $\beta_A = 1$. Through extensive numerical simulations, we find that the effectiveness of the proposed TFA strategy would not be qualitatively affected by the adoption of other values of α_A and β_A. We set $\alpha_B/\alpha_A < 1$ (i.e., $\alpha_B \leqslant 1$) here, which indicates that a journey on the high-speed layer B is favored compared with a journey on layer A. From Figs. 2(a) and 2(b), it can be found that for different values of β_B, both the order parameter H and average delivery time of packets $\langle T\rangle$ monotonically increase with R. Above the threshold R_c, H and $\langle T\rangle$ are finite, and they increase with R. More importantly, it is found that R_c exhibits a nonmonotonously varying with β_B, as shown in Fig. 2(c). Moreover, there is an optimal value $\beta_B^o(\alpha_B) = 0.7$ at which the traffic capacity R_c reaches the maximum value $R_c^o(\alpha_B) = 79$ when $\alpha_B = 0.5$. The average length of efficient paths $\langle d\rangle$ reaches the minimum value at the same parameters [see Fig. 3(c)]. Specifically, R_c first increases with β_B, peaks at $\beta_B^o(\alpha_B) = 0.7$, and then decreases. For a routing strategy, a higher R_c means more packets could be transported to their destinations without congestion, i.e., the larger R_c, the better the strategy. From the inset of Fig. 2(c), we see that there is an optimal value of $R_c^o = 32$ at $\beta_A \approx 1.0$ for a single network layer A without coupling with network layer B. Compared with the single network A, the optimal value R_c^o of the multilayer routing strategy is more than twice as much as that of the single-layer routing strategy. Even when β_B is between 0 and 1.5 in Fig. 2(c), R_c for the multilayer network is greater than that for the single network A, which means the multilayer routing strategy has a higher delivering efficiency than the single-layer routing strategy. The semianalytical predictions from Eq. (7) agree with the numerical values of R_c.

To understand the nonmonotonous phenomenon, we need to check what happens when the value of β_B varies. When β_B is small (large), the values of λ and δ are large (small) as shown in Figs. 3(a) and 3(b). It means that packets are more likely to be transported on layer B (A). For a small value of β_B, many coupled nodes are used to transport packets between two layers. Similarly to the effective strategy on monolayer networks, preferentially transporting the packets through middle-degree nodes in layer B could improve the traffic capacity of the system [29], and R_c thus first increases with β_B. For a large value of β_B, almost all of the packets are transported on layer A, which decreases the usage of coupled nodes in transporting the packets between two layers, and R_c thus decreases. In the case of large β_B [e.g., $\beta_B = 4.5$ in Fig. 2(c)], the traffic capacity will decrease to the $R_c = 32$ of monolayer A [see the inset of Fig. 2(c)], which is much smaller than $R_c^o(\alpha_B) = 79$ at $\beta_B^o(\alpha_B) = 0.7$ when $\alpha_B = 0.5$.

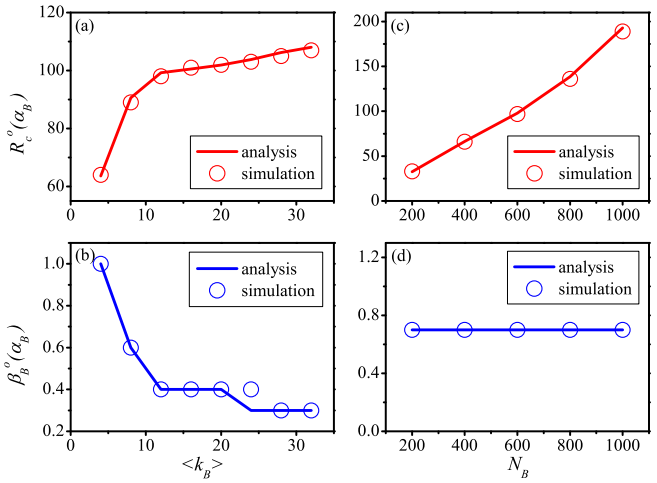

FIG. 4. The performance of the TFA strategy on artificial multilayer networks with different $\langle k_B\rangle$ and N_B. The maximum capacity $R_c^o(\alpha_B)$ (top) and the corresponding optimal microlevel parameter $\beta_B^o(\alpha_B)$ (bottom) as a function of $\langle k_B\rangle$ [(a) and (b)] and N_B [(c) and (d)], respectively. We set the other parameters as $N_A = 1000$, $\gamma = 3.0$, $k_{\min} = 2$, $k_{\max} = \sqrt{N_A}$, $\alpha_A = 1$, $\beta_A = 1$, $\alpha_B = 0.5$, $N_B = 500$ (a, b), $\langle k_B\rangle = 6$ (c, d).

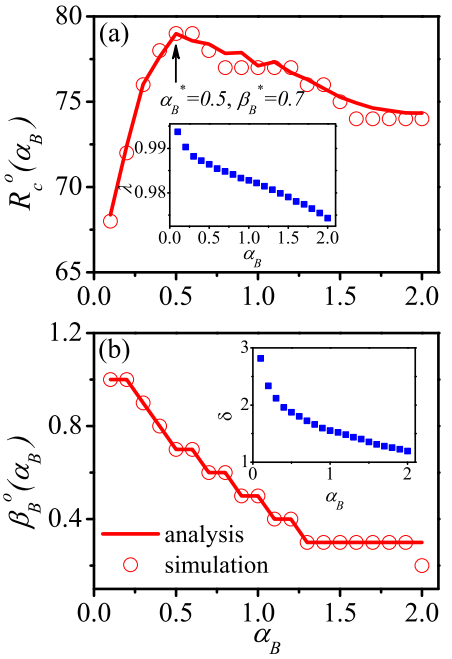

FIG. 5. The performance of the TFA strategy on artificial multilayer networks with different α_B. (a) $R_c^o(\alpha_B)$ and (b) $\beta_B^o(\alpha_B)$ as a function of α_B. The insets of panels (a) and (b), respectively, exhibit λ and δ versus α_B with $\beta_B = \beta_B^o(\alpha_B)$. We set the other parameters as $N_A = 1000$, $\gamma = 3.0$, $k_{\min} = 2$, $k_{\max} = \sqrt{N_A}$, $N_B = 500$, $\langle k_B\rangle = 6$, $\alpha_A = 1$, $\beta_A = 1$.

In Fig. 2(d), we further explore on which layer the congestion occurs more easily for different values of β_B. To this end, we set the transporting ability of nodes in layer A (B) as infinite, i.e., $C_A \to \infty$ [$C_B \to \infty$], to check the upper limit capacity of layer B (A). Since we set $C_A \to \infty$, congestion will occur only on layer B, and thus we can get the upper limit capacity R_B^u of layer B. Similarly, we can get the upper limit capacity R_A^u of layer A when we set $C_B \to \infty$. A multilayer network will reach its traffic capacity R_c once congestion occurs on any layer. That is to say, for a given β_B, R_c is the small one of R_A^u and R_B^u. From Fig. 2(d), we can obtain the R_c as a function of β_B in Fig. 2(c). It is found that congestion will first occur on layer B (A) with small (large) values of β_B, since layer B (A) has a smaller R_B^u (R_A^u). When $\beta_B = 0.7$, there are large values of R_A^u and R_B^u, which means that the traffic flow is reasonably allocated to layers A and B, and thus the TFA strategy shows a good performance with the maximum value of R_c. From what we discussed above, it can be observed that compared to the isolated low-speed network A, the capacity R_c of the multilayer network can be effectively improved at some parameters, because the traffic flow on the low-speed layer A is redistributed to the high-speed layer B reasonably. A larger capacity can be achieved by moderately transporting packets through small-degree nodes on the high-speed layer. The system capacity is affected by both layers A and B and depends nonmonotonically on β_B.

The effects of network size N_B and average degree $\langle k_B\rangle$ of layer B (i.e., the number of nodes and edges in the high-speed network) on system capacity are further investigated in Fig. 4. As shown in Figs. 4(a) and 4(c), it can be seen that when $\alpha_B = 0.5$, the maximum traffic capacity $R_c^o(\alpha_B)$ increases with $\langle k_B\rangle$ and N_B, since the number of efficient paths (coupled nodes) increases, i.e., increasing the size and average degree of the high-speed layer can enhance the traffic capacity of multilayer networks effectively. Meanwhile, it can be noted that when $\alpha_B = 0.5$ the optimal microlevel parameter $\beta_B^o(\alpha_B)$ decreases with $\langle k_B\rangle$ [see Fig. 4(b)] but does not change with N_B [see Fig. 4(d)], i.e., on the high-speed layer, the preference for packets to be transported through small-degree decreases with the increasing number of coupled nodes. Again, our semianalytical predictions agree with the numerical simulations.

All results above are obtained when $\alpha_B = 0.5$. As shown in Fig. 5, $R_c^o(\alpha_B)$ fluctuates with the varying of α_B. It can be observed that $R_c^o(\alpha_B)$ depends nonmonotonically on α_B [$R_c^o(\alpha_B)$ first increases and then decreases with α_B]. Moreover, it can be seen that the corresponding optimal microlevel parameter $\beta_B^o(\alpha_B)$ monotonically decreases with α_B, and the packets properly prefer to be transported via layer B. Thus, on the high-speed layer, the preference for packets to be transported via small-degree nodes increases with the packet-transporting speed. For small or large values of α_B, λ and δ are large or small as shown in the insets of Figs. 5(a) and 5(b), respectively. More importantly, we find that the system reaches the maximum traffic capacity $R_c^\star$ at both the optimal macrolevel parameter $\alpha_B^\star$ and microlevel parameter $\beta_B^\star$, and the number of transported packets by each layer reaches a balance. From Figs. 5(a) and 5(b), it can be obtained that $R_c^\star = 79$ at $(\alpha_B^\star, \beta_B^\star) = (0.5, 0.7)$. Without the high-speed network B, the maximum traffic capacity of a low-speed network is about 32 [see the inset of Fig. 2(b)]. The maximum traffic capacity of the system can be improved about 2.5 times once the network B is introduced. Although establishing high-speed transportation can improve the traffic capacity of low-speed network, our results indicate that a reasonable redistribution

TABLE I. Structural properties of the real-world networks, including number of nodes N, number of edges E, mean degree $\langle k\rangle$, maximum degree $k_{\max}$, degree heterogeneity $H_k = \langle k^2\rangle/\langle k\rangle^2$ [71], diameter D, average shortest distance L, correlation coefficient r [72], and clustering coefficient c [73].

Network	N	E	$\langle k\rangle$	$k_{\max}$	H_k	D	L	r	c
Railway	2125	3388	3.2	23	1.4	82	22.5	0.186	0.34
Airline	92	585	12.7	72	2.3	4	2.0	−0.448	0.69
Work	60	194	6.5	27	1.7	4	2.4	−0.218	0.64
Facebook	32	124	7.8	15	2.3	4	2.0	0.003	0.54

of traffic flow is an essential issue. The semianalytical predictions agree with the numerical simulations.

C. Real-world networks

A wide range of systems in the real world have multiple subsystems and layers of connectivity, which can be described as multilayer networks [41,42]. We verify the effectiveness of our proposed TFA strategy on two real-world multilayer networks. One of them is the Chinese Railway-Airline transportation network [67], and another one is the Work-Facebook relationship network of Employees of Computer Science Department (ECSD) at Aarhus University [70]. In the Railway-Airline coupled networks, we choose the Railway network as layer A and the Airline network as layer B; in the Work-Facebook coupled networks, we choose the Work network as layer A and the Facebook network as layer B. Some structural properties of the networks are presented in Table I.

In Fig. 6 the effectiveness of the TFA strategy on the Railway-Airline and Work-Facebook coupled networks is studied. Because of the extremely complicated structures of the networks, there are two peaks of R_c versus β_B, at

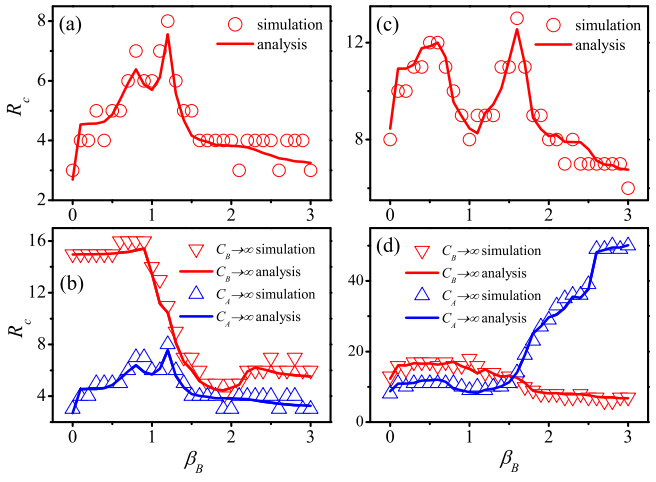

FIG. 6. The performance of the TFA strategy on real-world multilayer networks with $\alpha_B = 0.5$. (a) The traffic capacity R_c, and (b) the upper limit capacity of layer A and layer B as a function of the β_B on the Railway-Airline coupled networks. (c) and (d) The situations on the Work-Facebook coupled networks. We set $\alpha_A = 1$, $\beta_A = 1$, and $\alpha_B = 0.5$.

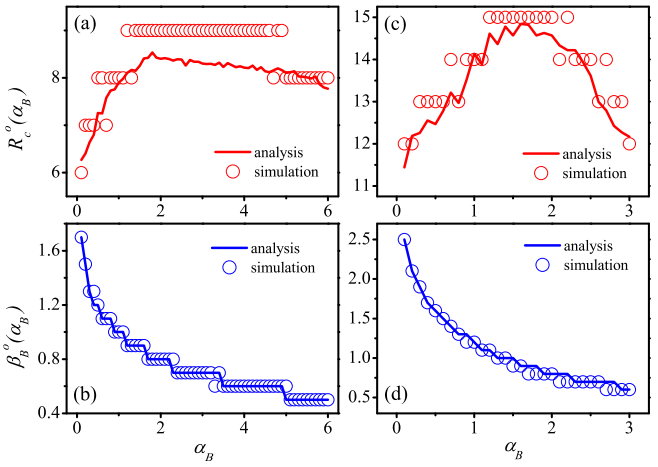

FIG. 7. The performance of the TFA strategy on real-world multilayer networks with different α_B. (a) The maximum capacity $R_c^o(\alpha_B)$ for a given α_B, and (b) the corresponding optimal microlevel parameter $\beta_B^o(\alpha_B)$ as a function of macrolevel parameter α_B on the Railway-Airline coupled networks. (c, d) The situations on the Work-Facebook coupled networks. We set $\alpha_A = 1$, and $\beta_A = 1$.

which the traffic capacity is very large, and $R_c^o(\alpha_B)$ corresponds to the second peak. Especially for the Work-Facebook coupled networks, two obvious peaks are observed in Fig. 6(c), which possibly result from the intralayer community structures and interlayer degree correlations of the Work-Facebook coupled networks. The Airline (Facebook) layer could reasonably redistribute the traffic flow of the Railway (Work) layer in an appropriate parameter range (e.g., $\beta_B = 1.2$ for Railway-Airline and $\beta_B = 1.6$ for Work-Facebook coupled networks), and the capacity R_c of two-coupled networks is improved when the Airline (Facebook) network joins in the system [see Figs. 6(a) and 6(c)]. The capacity of the Work-Facebook multilayer network is affected by both Work and Facebook networks [see Fig. 6(d)]. An interesting phenomenon is that the capacity of Railway-Airline coupled networks is always limited by the Airline layer [see Fig. 6(c)], because that too much traffic flow is redistributed to the Airline layer, thus exceeding its transporting ability (i.e., C_B). Therefore, it can be concluded that increasing the value of C_B may effectively enhance the capacity of system.

In Fig. 7 it can be seen that $R_c^o(\alpha_B)$ versus α_B exhibits a nonmonotonic pattern [see Figs. 7(a) and 7(c)], and the corresponding optimal microlevel parameter $\beta_B^o(\alpha_B)$ monotonically decreases with α_B [see Figs. 7(b) and 7(d)]. Similar to the artificial networks, we find that the systems reach their maximum traffic capacities at a certain combination of microlevel and macrolevel parameters. The fluctuations of curves in Figs. 6 and 7 are caused by the extremely complicated structures of real-world two-coupled networks. It should be noted that the semianalytical predictions qualitatively agree with the numerical simulations.

V. DISCUSSION

To alleviate the congestion on a low-speed transportation network, an intuitive way is to build a new high-speed network

in busy regions or among the high-flow nodes. Then the low- and high-speed networks constitute a multilayer network. For the purpose of improving the capacity of multilayer networks, reasonably redistributing the traffic flow is an essential issue and full of challenges. In this work, we first proposed a multilayer traffic-flow assignment (TFA) strategy by considering different transporting speeds of layers from the macrolevel view (by adjusting an macrolevel parameter α_F) and different roles of nodes from the perspective of microlevel structure (controlled by an adjustable microlevel parameter β_F). We then performed extensive numerical simulations on both artificial and real-world networks. It was found that the TFA strategy can redistribute the traffic flow on a low-speed layer to a high-speed layer reasonably. In particular, preferentially transporting the packets through small-degree nodes on the high-speed layer can enhance the traffic capacity of the system. And on the high-speed layer, the preference of packets to be transported via small-degree nodes should decrease with the network size and increase with the packet-transporting speed. In addition, we also found that the traffic capacity of multilayer networks can be improved by increasing the network size and the average degree of the high-speed layer. Moreover, the system capacity is affected by both layers A and B and depends nonmonotonically on β_B and α_B. With the optimal macrolevel $\alpha_B^\star$ and microlevel parameter $\beta_B^\star$, a given multilayer network can achieve the maximum traffic capacity $R_c^\star$. The semianalytical predictions agree with the numerical simulations on both artificial and real-world networks.

A wise way to alleviate traffic congestion on multilayer networks is designing effective traffic-flow assignment strategy. Our results exhibited a way to reasonably redistribute the traffic flow. In this work, we proposed an effective flow assignment strategy based on the consideration of the local structures of different nodes and the transporting speeds of different layers. We validated our proposed strategy on multilayer networks including two layers, and it was proved that our proposed strategy can effectively improve the traffic capacity of multilayer networks. Our research may stimulate future studies on designing realistic transportation and communication multilayer networks, such as considering different structural characteristics, origin-destination allocations of packets and transporting abilities of nodes, limited traffic resources, transporting cost of layers, and multilayer networks with more than two layers.

ACKNOWLEDGMENTS

This work was supported by the National Natural Science Foundation of China (Grant Nos. 11575041 and 61703330), the Natural Science Foundation of Shanghai (Grant No. 18ZR1412200), and the Science and Technology Commission of Shanghai Municipality (Grant No. 18dz2271000). We would like to acknowledge gratefully Prof. Da-Ren He and Prof. Chang-Gui Gu and associate professor Xiu-Lian Xu, from whom we got much guidance as well as data for the Chinese Railway-Airline network.

[1] S. H. Strogatz, Nature (London) **410**, 268 (2001).
[2] R. Albert and A.-L. Barabási, Rev. Mod. Phys. **74**, 47 (2002).
[3] M. Newman, *Networks: An Introduction* (Oxford University Press, Oxford, 2010).
[4] A.-L. Barabási, *Network Science* (Cambridge University Press, Cambridge, 2016).
[5] A. Arenas, A. Díaz-Guilera, and R. Guimerá, Phys. Rev. Lett. **86**, 3196 (2001).
[6] A. E. Motter, Phys. Rev. Lett. **93**, 098701 (2004).
[7] L. Zhao, Y.-C. Lai, K. Park, and N. Ye, Phys. Rev. E **71**, 026125 (2005).
[8] Z. Wu, L. A. Braunstein, S. Havlin, and H. E. Stanley, Phys. Rev. Lett. **96**, 148702 (2006).
[9] M. Barthélemy, Phys. Rep. **499**, 1 (2011).
[10] J. Wu, H. Sun, D. Z. Wang, M. Zhong, L. Han, and Z. Gao, Transport. Res. C **31**, 73 (2013).
[11] J.-Q. Dong, Z.-G. Huang, Z. Zhou, L. Huang, Z.-X. Wu, Y. Do, and Y.-H. Wang, Europhys. Lett. **99**, 20007 (2012).
[12] Z.-Y. Jiang, M.-G. Liang, S. Zhang, S.-J. Wang, and D.-C. Guo, Int. J. Mod. Phys. C **23**, 1250065 (2012).
[13] J.-F. Zheng, Z.-H. Zhu, H.-M. Du, and Z.-Y. Gao, Int. J. Mod. Phys. C **24**, 1350072 (2013).
[14] A. Huang, G. Zang, Z. He, and W. Guan, Int. J. Mod. Phys. B **31**, 1750087 (2017).
[15] G. Chen, S.-X. Wang, L.-W. Wu, P. Mei, X.-H. Yang, and G.-H. Wen, Europhys. Lett. **116**, 66001 (2017).
[16] X. Yang, J. Li, C. Pu, M. Yan, R. R. Sharafat, J. Yang, K. Gakis, and P. M. Pardalos, Phys. Rev. E **95**, 012322 (2017).
[17] X. Zhang, Z. Zhou, and D. Cheng, PLoS ONE **12**, e0172035 (2017).
[18] R. Guimerà, A. Arenas, A. Díaz-Guilera, and F. Giralt, Phys. Rev. E **66**, 026704 (2002).
[19] R. Guimerà, A. Díaz-Guilera, F. Vega-Redondo, A. Cabrales, and A. Arenas, Phys. Rev. Lett. **89**, 248701 (2002).
[20] S. Boccaletti, V. Latora, Y. Moreno, M. Chavez, and D.-U. Hwang, Phys. Rep. **424**, 175 (2006).
[21] B. Danila, Y. Yu, J. A. Marsh, and K. E. Bassler, Phys. Rev. E **74**, 046106 (2006).
[22] B. Danila, Y. Yu, J. A. Marsh, and K. E. Bassler, Chaos **17**, 026102 (2007).
[23] Z. Liu, M.-B. Hu, R. Jiang, W.-X. Wang, and Q.-S. Wu, Phys. Rev. E **76**, 037101 (2007).
[24] G.-Q. Zhang, D. Wang, and G.-J. Li, Phys. Rev. E **76**, 017101 (2007).
[25] G. Li, S. D. S. Reis, A. A. Moreira, S. Havlin, H. E. Stanley, and J. S. Andrade Jr., Phys. Rev. Lett. **104**, 018701 (2010).
[26] Y. Xia and D. Hill, Europhys. Lett. **89**, 58004 (2010).
[27] L. Xiang, H. Mao-Bin, L. Jian-Cheng, D. Jian-Xun, and S. Qin, Chin. Phys. B **22**, 018904 (2013).
[28] G.-Q. Zhang, S. Zhou, D. Wang, G. Yan, and G.-Q. Zhang, Physica A **390**, 387 (2011).
[29] G. Yan, T. Zhou, B. Hu, Z.-Q. Fu, and B.-H. Wang, Phys. Rev. E **73**, 046108 (2006).
[30] D. De Martino, L. Dall'Asta, G. Bianconi, and M. Marsili, Phys. Rev. E **79**, 015101(R) (2009).

[31] M. Tang, Z. Liu, X. Liang, and P. M. Hui, Phys. Rev. E **80**, 026114 (2009).
[32] B. Tadić and M. Mitrović, Eur. Phys. J. B **71**, 631 (2009).
[33] X. Ling, M.-B. Hu, R. Jiang, and Q.-S. Wu, Phys. Rev. E **81**, 016113 (2010).
[34] A. Rachadi, M. Jedra, and N. Zahid, Chaos **23**, 013114 (2013).
[35] Y. Gan, M. Tang, and H. Yang, Eur. Phys. J. B **86**, 1 (2013).
[36] P. Echenique, J. Gómez-Gardenes, and Y. Moreno, Europhys. Lett. **71**, 325 (2005).
[37] Z.-X. Wu, W.-X. Wang, and K.-H. Yeung, New J. Phys. **10**, 023025 (2008).
[38] W.-X. Wang, Z.-X. Wu, R. Jiang, G. Chen, and Y.-C. Lai, Chaos **19**, 033106 (2009).
[39] M. Bayati, C. Borgs, A. Braunstein, J. Chayes, A. Ramezanpour, and R. Zecchina, Phys. Rev. Lett. **101**, 037208 (2008).
[40] C. H. Yeung, D. Saad, and K. Wong, Proc. Natl. Acad. Sci. USA **110**, E13717 (2013).
[41] M. Kivelä, A. Arenas, M. Barthelemy, J. P. Gleeson, Y. Moreno, and M. A. Porter, J. Compl. Netw. **2**, 203 (2014).
[42] S. Boccaletti, G. Bianconi, R. Criado, C. I. Del Genio, J. Gómez-Gardeñes, M. Romance, I. Sendiña-Nadal, Z. Wang, and M. Zanin, Phys. Rep. **544**, 1 (2014).
[43] S. V. Buldyrev, R. Parshani, G. Paul, H. E. Stanley, and S. Havlin, Nature (London) **464**, 1025 (2010).
[44] W. Wang, M. Tang, H. Yang, Y. Do, Y.-C. Lai, and G. Lee, Sci. Rep. **4**, 5097 (2014).
[45] J. Gómez-Gardenes, I. Reinares, A. Arenas, and L. M. Floría, Sci. Rep. **2**, 620 (2012).
[46] J. Aguirre, R. Sevilla-Escoboza, R. Gutiérrez, D. Papo, and J. M. Buldú, Phys. Rev. Lett. **112**, 248701 (2014).
[47] X.-L. Chen, R.-J. Wang, M. Tang, S.-M. Cai, H. E. Stanley, and L. A. Braunstein, New J. Phys. **20**, 013007 (2018).
[48] Y. Zhuo, Y. Peng, C. Liu, Y. Liu, and K. Long, Physica A **390**, 2401 (2011).
[49] Y. Zhuo, Y. Peng, X. Yang, and K. Long, Phys. Scr. **84**, 055802 (2011).
[50] Z.-Y. Jiang, M.-G. Liang, S. Zhang, W. Zhou, and H. Jin, Int. J. Mod. Phys. C **24**, 1350051 (2013).
[51] S. Zhang, M.-G. Liang, Z.-Y. Jiang, and H.-J. Li, Int. J. Mod. Phys. C **26**, 1550001 (2015).
[52] C. Pu, S. Li, X. Yang, J. Yang, and K. Wang, Physica A **447**, 261 (2016).
[53] J. Ma, W. Han, Q. Guo, S. Zhang, J. Wang, and Z. Wang, Int. J. Mod. Phys. C **27**, 1650044 (2016).
[54] Z. Fan and W. K. Tang, Physica A **456**, 327 (2016).
[55] D. Li, B. Fu, Y. Wang, G. Lu, Y. Berezin, H. E. Stanley, and S. Havlin, Proc. Natl. Acad. Sci. USA **112**, 669 (2015).
[56] W.-B. Du, X.-L. Zhou, O. Lordan, Z. Wang, C. Zhao, and Y.-B. Zhu, Transport. Res. E **89**, 108 (2016).
[57] R. G. Morris and M. Barthélemy, Phys. Rev. Lett. **109**, 128703 (2012).
[58] J. Zhou, G. Yan, and C.-H. Lai, Europhys. Lett. **102**, 28002 (2013).
[59] O. Yagan, D. Qian, J. Zhang, and D. Cochran, IEEE J. Sel. Areas Commun. **31**, 1038 (2013).
[60] F. Tan, J. Wu, Y. Xia, and C. K. Tse, Phys. Rev. E **89**, 062813 (2014).
[61] A. Solé-Ribalta, S. Gómez, and A. Arenas, Phys. Rev. Lett. **116**, 108701 (2016).
[62] M. Li, M.-B. Hu, and B.-H. Wang, Sci. Rep. **6**, 39175 (2016).
[63] W.-B. Du, X.-L. Zhou, Z. Chen, K.-Q. Cai, and X.-B. Cao, Chaos Soliton. Fract. **68**, 72 (2014).
[64] W.-B. Du, X.-L. Zhou, M. Jusup, and Z. Wang, Sci. Rep. **6**, 19059 (2016).
[65] S. Manfredi, E. Di Tucci, and V. Latora, Phys. Rev. Lett. **120**, 068301 (2018).
[66] A. Solé-Ribalta, A. Arenas, and S. Gómez, New J. Phys. **21**, 035003 (2019).
[67] C.-G. Gu, S.-R. Zou, X.-L. Xu, Y.-Q. Qu, Y.-M. Jiang, D. R. He, and H.-K. Liu, T. Zhou, Phys. Rev. E **84**, 026101 (2011).
[68] M. Catanzaro, M. Boguñá, and R. Pastor-Satorras, Phys. Rev. E **71**, 027103 (2005).
[69] P. Erdös and A. Rényi, Publ. Math. Inst. Hungar. Acad. Sci **5**, 17 (1960).
[70] M. Magnani, B. Micenkova, and L. Rossi, arXiv:1303.4986.
[71] R. Pastor-Satorras and A. Vespignani, Phys. Rev. Lett. **86**, 3200 (2001).
[72] M. E. J. Newman, Phys. Rev. Lett. **89**, 208701 (2002).
[73] D. J. Watts and S. H. Strogatz, Nature (London) **393**, 440 (1998).